

HDD

BBC

ENGINEERING DIVISION

MONOGRAPH

NUMBER 36: APRIL 1961

Some Aspects of Optical Lens Performance

Secondary Flare in Lenses

by

K. HACKING, B.Sc.

The Design of Lens Hoods

by

W. N. SPROSON, M.A.

BRITISH BROADCASTING CORPORATION

PRICE FIVE SHILLINGS



BBC ENGINEERING MONOGRAPH

No. 36

SOME ASPECTS OF OPTICAL LENS PERFORMANCE

PART I: SECONDARY FLARE IN LENSES

by

K. Hacking, B.Sc.

PART II: THE DESIGN OF LENS HOODS

by

W. N. Sproson, M.A.

APRIL 1961

BRITISH BROADCASTING CORPORATION

FOREWORD

THIS is one of a series of Engineering Monographs published by the British Broadcasting Corporation. About six are produced every year, each dealing with a technical subject within the field of television and sound broadcasting. Each Monograph describes work that has been done by the Engineering Division of the BBC and includes, where appropriate, a survey of earlier work on the same subject. From time to time the series may include selected reprints of articles by BBC authors that have appeared in technical journals. Papers dealing with general engineering developments in broadcasting may also be included occasionally.

This series should be of interest and value to engineers engaged in the fields of broadcasting and of telecommunications generally.

Individual copies cost 5s. post free, while the annual subscription is £1 post free. Orders can be placed with newsagents and booksellers, or BBC PUBLICATIONS, 35 MARYLEBONE HIGH STREET, LONDON, W.1.

CONTENTS

<i>Section</i>	<i>Title</i>	<i>Page</i>
	PREVIOUS ISSUES IN THIS SERIES	4
PART I SECONDARY FLARE IN LENSES		
	SUMMARY	5
1.	INTRODUCTION	5
2.	VEILING-GLARE INDEX	6
2.1	Method of Measurement	6
2.2	Mode of Operation	7
2.3	Patch Size	7
2.4	Effect of Short Object-distance	9
3.	TRANSMISSION AND ABSORPTION	9
4.	THEORETICAL RELATIONSHIP BETWEEN VEILING-GLARE AND TRANSMISSION FACTOR	9
4.1	Theoretical Derivation	9
4.2	Quality Index for Lens Design	11
5.	RESULTS	11
5.1	Veiling-glare Index	11
5.2	Effect of Aperture on the Veiling-glare Index	11
6.	DISTRIBUTION OF FLARE LIGHT IN THE IMAGE PLANE	11
6.1	Method of Investigation	11
6.2	Results	12
7.	SURFACE DUST AND FINGERPRINTS	13
7.1	Method of Investigation	13
7.2	Results	13
7.3	Earlier Results with Dust Layers	13
8.	CONCLUSIONS	13
PART II THE DESIGN OF LENS HOODS		
	SUMMARY	15
9.	INTRODUCTION	15
10.	BASIC CONSIDERATIONS	15
10.1	Length of Hood	15
10.2	Partial and Complete Protection	16
10.3	Shape of Lens Hood	16
11.	PROTECTION ANGLES	17
12.	EFFECT OF UNUSUAL LENS DESIGNS	17
13.	CONCLUSIONS	19
14.	REFERENCES	19

PREVIOUS ISSUES IN THIS SERIES

No.	Title	Date
1.	<i>The Suppressed Frame System of Telerecording</i>	JUNE 1955
2.	<i>Absolute Measurements in Magnetic Recording</i>	SEPTEMBER 1955
3.	<i>The Visibility of Noise in Television</i>	OCTOBER 1955
4.	<i>The Design of a Ribbon Type Pressure-gradient Microphone for Broadcast Transmission</i>	DECEMBER 1955
5.	<i>Reproducing Equipment for Fine-groove Records</i>	FEBRUARY 1956
6.	<i>A V.H.F./U.H.F. Field-strength Recording Receiver using Post-detector Selectivity</i>	APRIL 1956
7.	<i>The Design of a High Quality Commentator's Microphone Insensitive to Ambient Noise</i>	JUNE 1956
8.	<i>An Automatic Integrator for Determining the Mean Spherical Response of Loudspeakers and Microphones</i>	AUGUST 1956
9.	<i>The Application of Phase-coherent Detection and Correlation Methods to Room Acoustics</i>	NOVEMBER 1956
10.	<i>An Automatic System for Synchronizing Sound on Quarter-inch Magnetic Tape with Action on 35-mm Cinematograph Film</i>	JANUARY 1957
11.	<i>Engineering Training in the BBC</i>	MARCH 1957
12.	<i>An Improved 'Roving Eye'</i>	APRIL 1957
13.	<i>The BBC Riverside Television Studios: The Architectural Aspects</i>	JULY 1957
14.	<i>The BBC Riverside Television Studios: Some Aspects of Technical Planning and Equipment</i>	OCTOBER 1957
15.	<i>New Equipment and Methods for the Evaluation of the Performance of Lenses for Television</i>	DECEMBER 1957
16.	<i>Analysis and Measurement of Programme Levels</i>	MARCH 1958
17.	<i>The Design of a Linear Phase-Shift Low-pass Filter</i>	APRIL 1958
18.	<i>The BBC Colour Television Tests: An Appraisal of Results</i>	MAY 1958
19.	<i>A U.H.F. Television Link for Outside Broadcasts</i>	JUNE 1958
20.	<i>The BBC's Mark II Mobile Studio and Control Room for the Sound Broadcasting Service</i>	AUGUST 1958
21.	<i>Two New BBC Transparencies for Testing Television Camera Channels</i>	NOVEMBER 1958
22.	<i>The Engineering Facilities of the BBC Monitoring Service</i>	DECEMBER 1958
23.	<i>The Crystal Palace Band I Television Transmitting Aerial</i>	FEBRUARY 1959
24.	<i>The Measurement of Random Noise in the presence of a Television Signal</i>	MARCH 1959
25.	<i>A Quality-Checking Receiver for V.H.F. F.M. Sound Broadcasting</i>	JUNE 1959
26.	<i>Transistor Amplifiers for Sound Broadcasting</i>	AUGUST 1959
27.	<i>The Equipment of the BBC Television Film Studios at Ealing</i>	JANUARY 1960
28.	<i>Programme Switching, Control, and Monitoring in Sound Broadcasting</i>	FEBRUARY 1960
29.	<i>A Summary of the Present Position of Stereophonic Broadcasting</i>	APRIL 1960
30.	<i>Film Processing and After-processing Treatment of 16-mm Films</i>	MAY 1960
31.	<i>The Power Gain of Multi-Tiered V.H.F. Transmitting Aerials</i>	JULY 1960
32.	<i>A New Survey of the BBC Experimental Colour Transmissions</i>	OCTOBER 1960
33.	<i>Sensitometric Control in Film Making</i>	DECEMBER 1960
34.	<i>A Mobile Laboratory for UHF and VHF Television Surveys</i>	FEBRUARY 1961
35.	<i>Tables of Horizontal Radiation Patterns of Dipoles Mounted on Cylinders</i>	FEBRUARY 1961

SECONDARY FLARE IN LENSES

SUMMARY

The image formed by a lens is often reduced in contrast by extraneous light spread extensively over the image plane as a result of specular interfacial reflections within the lens and scattering by surface irregularities. A method of measuring the magnitude of the flare light is described. The theoretical relationship between the transmission factor of the lens and the flare component due to specular reflections is discussed. The non-uniform distribution of flare has been investigated experimentally and the importance of lens cleanliness has been demonstrated. The average results of flare measurements on a number of lenses used in television applications are given.

1. Introduction

Suppose that we have a well-defined patch of light as an object in an otherwise dark field. An ideal lens system would produce a faithful image (reduced or magnified in size) of this object. The image would be equally well-defined and contain all the light emerging from the lens. In practice, of course, this does not happen and there is a 'spread' of light outside the confines of the ideal image. The amount of scattered light is usually small, but not insignificant, and the edges of the image appear to be 'flared'.

Fig. 1 illustrates the spread of light in the image of an illuminated slot of width about 1/30th of the working field of the lens. The intensity profile across the field might be roughly as shown by the full line in the figure (the intensity scale used is logarithmic in order to demonstrate the effect more clearly). The light spreading or flaring out from the image of the slot may be regarded as the sum of two components (termed the primary and secondary flare components). These are indicated separately by the shaded areas in the figure.

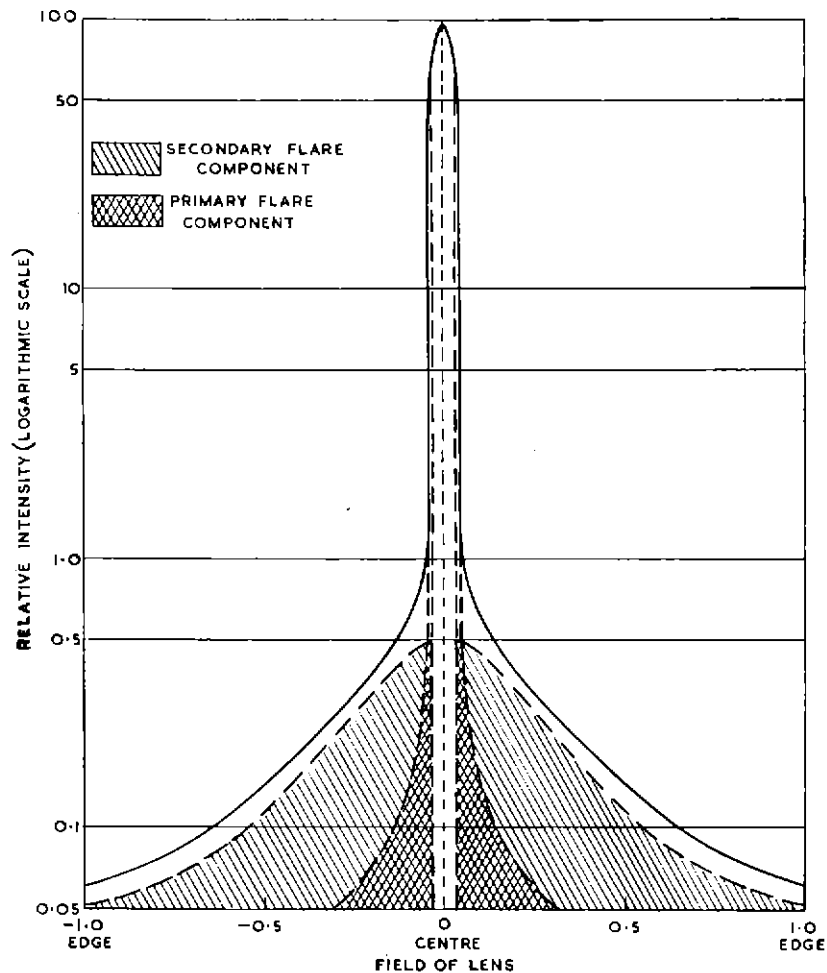


Fig. 1 — Illustrating the general synthesis of the spread function for a badly corrected lens imaging an axial illuminated slit 1/30th of the field width

Primary flare is due to refractive defects associated with the lens design, such as spherical and comatic aberrations. If the lens is badly corrected the primary flare component might be severe (as suggested in Fig. 1 for instance). In well-corrected lenses the reduction of contrast in very coarse detail due to primary flare is usually small compared with that due to secondary flare, but for fine detail the reverse is true. Primary flare will not be considered further in this monograph.

The secondary flare component of the intensity profile arises in two distinct ways. Firstly, there is a spread of light due to specular reflection at the glass/air surfaces. (The cemented boundaries between glass elements which differ in refractive index also reflect specularly but to a negligible extent because the change in index is usually small.) Light which has been reflected from two or more surfaces subsequently finds its way into the image space, where it is distributed widely. However, in spite of the complexity of the interfacial reflections which must occur in multi-element lenses, the light reflected in this way is not necessarily spread uniformly over the image plane. This non-uniformity is greatly accentuated by light spread, arising from the second cause—scattering by surface irregularities at both glass/air and glass/glass interfaces. These irregularities often take the form of surface scratches, dust particles, pitting caused by erosion, cement imperfections, crazing of the anti-reflection coatings, or greasy organic surface deposits such as fingerprints. Referring again to the imaging of a small illuminated object-patch, it is found that the scattered light due to surface imperfections is concentrated around the image of the patch, and that its intensity decreases quickly as one moves away from the patch.

The distribution of secondary flare light in photographic objectives has been investigated by Guild,¹ and is also briefly described in Section 6 of this monograph. In ordinary scenes where many highlight patches are distributed over a large area of the total working field of the lens, the integrated effect of secondary flare from individual light patches is to produce a fairly uniform veil of non-image-forming light which has been termed veiling-glare.¹ Secondary flare gives rise to a depression of the overall frequency response characteristic of the lens at all but the very lowest spatial frequencies. The maximum contrast in the image of a scene will be limited to a value determined by the ratio of the mean brightness to the peak brightness of the scene (i.e. the 'key' of the scene). The maximum contrast will decrease as this ratio increases.

An additional cause of flare, which must also be mentioned, is reflection from the unblackened parts of the lens mount and iris diaphragm. The reflected light is sometimes crudely focused in the image plane, so producing flare spots or 'ghost' images of the offending parts.

2. Veiling-glare Index

2.1 Method of Measurement

The amount of veiling-glare produced by a lens system provides a useful measure of its secondary flare characteristic. It is convenient to design the measuring apparatus to simulate conditions which give directly the maximum amount of veiling-glare likely to be encountered in practice (excluding extreme cases such as a bright source of light in the object-field). This situation is obtained when almost the whole of the working object-field is uniformly illuminated.

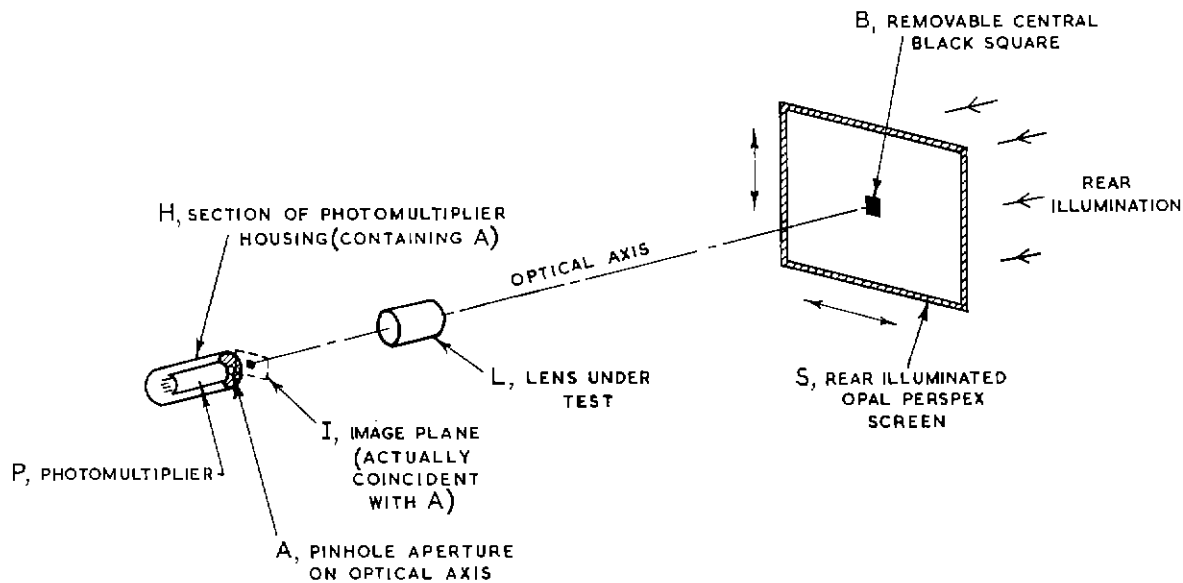


Fig. 2 — Veiling-glare measurement

Fig. 2 shows a simple arrangement which has been adopted for the measurement of veiling-glare. S is a rear-illuminated diffusing screen which is placed normal to the optical axis of the lens L under test. The screen is symmetrically placed with respect to the optical axis and provision is made for manual adjustment in both horizontal and vertical directions, as indicated in the figure. A sensitive photomultiplier P, in a metal housing H, is placed behind the lens. The metal housing is light-tight except for a small pinhole A near the photo-cathode of the photomultiplier. The pinhole is arranged to lie on the optical axis of the lens, as shown in Fig. 2. The object-screen and lens under test are mounted on an optical bench (not shown) enabling their relative separations to be varied so that an image I, of the required size, can be formed on the plane containing the pinhole A. Means are provided whereby an opaque (square) black patch B can be introduced just in front of the illuminated object-screen S, with its centre on the optical axis of the lens.

The aspect ratio of the object-screen is 3:4 corresponding with normal television standards. The screen is illuminated with reasonable uniformity by a projector lamp, the brightness being controlled by means of an auto-transformer. The polar diagram of the screen is approximately that of a Lambert surface.

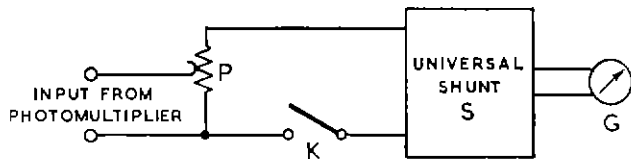


Fig. 3 — Galvanometer control arrangement

The e.h.t. unit supplying the photomultiplier dynode chain is stabilized. The output of the photomultiplier is coupled to a spot galvanometer G as indicated in Fig. 3, where P is a potentiometer, K is a simple switch-key and S is a universal shunt arrangement. The latter allows a $\times 10$ change of galvanometer sensitivity while maintaining critical damping.

The method consists of measuring the illumination (i.e. flux crossing image plane per unit area) at the centre of the image of the object-screen both with and without the central black patch. The ratio of these quantities is termed the veiling-glare index (usually expressed as a percentage). Using the apparatus described, this method amounts to recording two galvanometer readings and taking their ratio.

Fig. 4 shows a photograph of the latest equipment for measuring the veiling-glare index. This operates on the principles outlined above although there are some differences in instrumentation.

2.2 Mode of Operation

The lens to be tested is mounted on the optical bench and its position along the bench is adjusted, in conjunction

with that of the illuminated object-screen, so that an image filling the required format area is focused in the plane containing the pinhole. Small adjustments are then made to the horizontal and vertical positions of the object-screen with the black patch in situ. The galvanometer can be used to indicate correct centring by adjusting for a minimum deflection. The first recorded galvanometer reading is that for peak illumination (i.e. with black patch removed), the input potentiometer being adjusted so that a convenient deflection is obtained with the galvanometer in its most insensitive condition. The black patch is replaced and a second reading taken, with the galvanometer sensitivity increased if necessary. A lens cap is useful when taking the zero readings of the galvanometer.

If required, colour filters can be used to measure the veiling-glare index for a selected part of the visible spectrum. In this case it is better to place the filters either between the black patch and object-screen or between the pinhole aperture and the photomultiplier. The latter alternative is to be preferred.

2.3 Patch Size

Owing to the non-uniform distribution of secondary flare from small object-areas, it is necessary to state the size of the patch used when specifying the veiling-glare index because the latter depends on the size chosen. Fig. 5 shows the effect of patch size on the measured veiling-glare index for a telerecording lens having a focal length of 2 in. (50 mm). It will be seen that, for this particular lens, the measured veiling-glare index decreases linearly as the dimension of the square-shaped patch increases. In order to obtain near-maximum conditions for the veiling-glare index, it is necessary to use a small patch. On the other hand, if the patch size is too small, some primary flare will be included in the measurement.

A size of patch which bears a fixed ratio to that of the rectangular object-screen has been adopted. The patch area

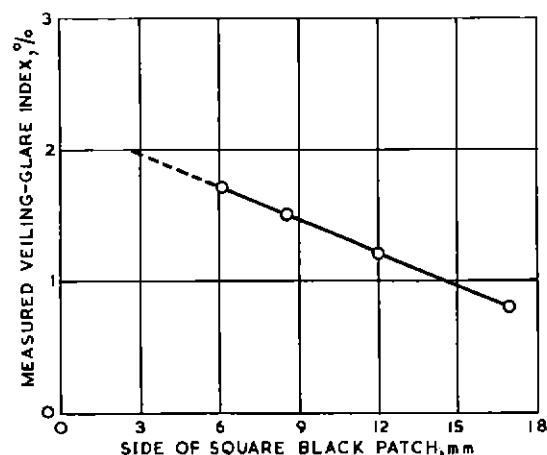


Fig. 5 — Effect of patch size on the measured veiling-glare index for a telerecording lens ($f=2$ in.). A patch size of 6 by 6 mm corresponds to 30 by 30 picture elements



Fig. 4 — Optical bench constructed for veiling-glare measurement

to screen area ratio is approximately 1 : 200, and when related to the British 405-line television standard the patch area is equivalent to 30 by 30 picture elements.

2.4 Effect of Short Object-distance

In order to simulate the practical condition in which veiling-glare is greatest, it is necessary to ensure that the diagonal of the object-screen subtends an angle at the lens which corresponds to the maximum angular field for which the lens is intended to be used. For instance, a lens intended for use in an image orthicon camera using a 40 mm diagonal format would require a maximum angular field given by $2 \tan^{-1} (20/f)$, where f is the focal length of the lens in mm. In describing earlier the mode of operation of the apparatus, it was stated that the object-screen is imaged by the lens so that the size of the image is that of the format for which the lens is intended to be used. This is done in order to maintain the 30 by 30 picture-element patch standard. Since, however, the image is not at the focal plane of the lens, because of the finite object-distance, the angle subtended at the lens by the object-screen is less than that ideally required. It can be shown that the area of the object-screen is smaller than that required by a factor $[1/(1+m)]^2$, where m is the ratio of the image-distance to the object-distance, ($m < 1$). This error could be serious for some lenses where the secondary flare is uniformly distributed over the image plane, so that the veiling-glare index is roughly proportional to the area of the illuminated screen. In fact, measurements on two types of lenses showed that the peripheral half of the total illuminated screen area accounts for only 10 per cent to 15 per cent of the veiling-glare index at the centre. Nevertheless, in order to determine the near-maximum veiling-glare index, it is preferable that m should be as small as possible, which means using as large an object-screen as possible.

The other practical alternative is to use a separate object-screen for each format size, each having the correct ratio of patch size to screen size. This ratio would be chosen in each case to make the image of the black patch correspond with 30 by 30 picture elements, while the illuminated area subtended the same angle at the lens as would be subtended by an object at infinity having an image corresponding to the required format.

3. Transmission and Absorption

The fraction of the incident light which a given lens transmits (i.e. its transmission factor) is related to the amount of secondary flare introduced by surface reflections. Knowledge of the transmission factor alone is insufficient to deduce the actual veiling-glare performance of the lens, but it can be useful in deriving an upper limit for the component of the veiling-glare index due to specular reflections. Clearly, if a lens had a high transmission factor it might be expected that secondary flare effects due to surface reflections would be small, and in the limit, if there were no secondary flare, the lens would have perfect transmission, i.e. $T=1-B$, where B is the absorption due to the lens elements and T the transmission factor.

The apparatus required to measure the transmission factor of a lens, for a small pencil of light incident along its optical axis, is relatively simple. All that is required is to determine, using a photocell, the amounts of incident and emergent light flux and determine the ratio of these quantities. Care should be taken to use the same area of the photocell for both readings. In this connection it has been found preferable to fix the photocell and light source on an optical bench, and take readings with and without the lens interposed. A position of the lens relative to the photocell can usually be found such that the cross-section of the light pencil at the photocell remains substantially unchanged when the lens is interposed.

It would be helpful to determine the proportion of the incident light flux absorbed by the lens or lens system. This quantity is, however, difficult to assess in practice because it entails measuring the light reflected by the lens in addition to that transmitted, and the methods available are somewhat complicated.

4. Theoretical Relationship Between Veiling-glare and Transmission Factor

An exact computation of the component of secondary flare due to specular reflections, for any given lens design, is possible, but it would be even more complicated than the already formidable task of its initial design. Nevertheless, it is possible to obtain a simplified general relationship between the measured transmission factor and the maximum veiling-glare index for a given number of glass/air interfaces, if causes of flare other than reflections are ignored.

4.1 Theoretical Derivation

Let us assume that a lens with N glass/air interfaces can be represented (as far as reflections are concerned) by a 'stack' of N plane parallel surfaces, each having a Fresnel transmission coefficient t , as shown schematically in Fig. 6. A beam of light of unit flux is incident normally on the first surface and a flux T_m (≤ 1) finally emerges from the 'stack'. T_m corresponds to the measured transmission factor. Since we are concerned with large path lengths, interference effects can be neglected, so that the separations of the N surfaces are immaterial.

The veiling-glare index, V , for an optical system is defined, in accordance with the method of measurement described earlier and in terms of the parameters shown in Fig. 5, as

$$V = \frac{T_m - t^N}{T_m} = 1 - \frac{t^N}{T_m} \dots \dots \dots (1)$$

if we assume that the flare and directly transmitted components of T_m would illuminate uniformly the same area of a hypothetical image plane.

It can be shown that, in so far as the total transmission is concerned, any two consecutive surfaces, such as 1 and 2

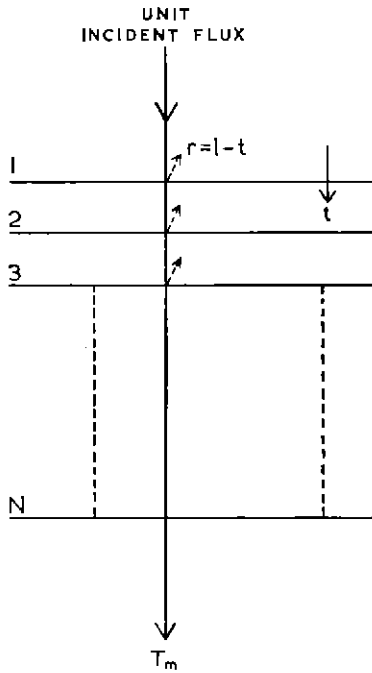


Fig. 6 — Hypothetical model of lens system for deducing upper limit of veiling-glare index

in Fig. 6, can be replaced by a single surface having a transmission coefficient given by $t/(2-t)$. In the same way N consecutive surfaces can be replaced by a single surface with a transmission coefficient given by

$$\frac{t}{N-(N-1)t}$$

Hence we have

$$T_m = \frac{t}{N-(N-1)t} \dots \dots \dots (2)$$

which can be re-arranged as

$$t = \frac{NT_m}{[1+(N-1)T_m]} \dots \dots \dots (3)$$

Substituting in equation 1 we have

$$V = 1 - \frac{N^N T_m^{N-1}}{[1+(N-1)T_m]^N} \dots \dots \dots (4)$$

which gives the veiling-glare index in terms of the transmission factor of the system and the number of reflecting surfaces. It can be shown that in the limit, when N tends to infinity, equation 4 becomes*

$$\lim_{N \rightarrow \infty} V = 1 - (1/T_m) e^{1-(1/T_m)} \dots \dots \dots (5)$$

Fig. 7 shows a plot of V against T_m , for $N=2, 4, 8, 16$, and ∞

*The author is indebted to Mr G. D. Monteath for pointing out the existence of this limit.

Real lens systems differ in three main ways from the theoretical model used to derive equations 4 and 5. These are:

- (a) The reflecting surfaces are far from being plane-parallel, so that some of the secondary flare light is directed towards the walls of the lens system and is mainly absorbed. Further, the number of inter-reflections is not infinite for the same reason.
- (b) The illumination due to the secondary flare component of the total emergent flux is not confined to the area illuminated by the image-forming component, neither is it necessarily uniform over the image plane. The flare light is in fact 'spread' over a greater area than that of the working field.
- (c) The theoretical derivation assumes that there is no loss of light energy due to absorption by the media between the reflecting surfaces. In practice there is absorption and it leads to a useful reduction in veiling-glare, but at the expense of a lower transmission factor. In most lenses the amount of absorption due to the glass elements is small, but one method of reducing veiling-glare would be to increase this absorption deliberately.

The three differences outlined above all tend to lower the veiling-glare index. Hence the theoretical expression given by equation 4 represents an upper limit for that component of the veiling-glare index which is due to specular reflections. Theoretically, equation 4 is useful because it can form the basis for assessing the quality of a given lens design from the point of view of veiling-glare.

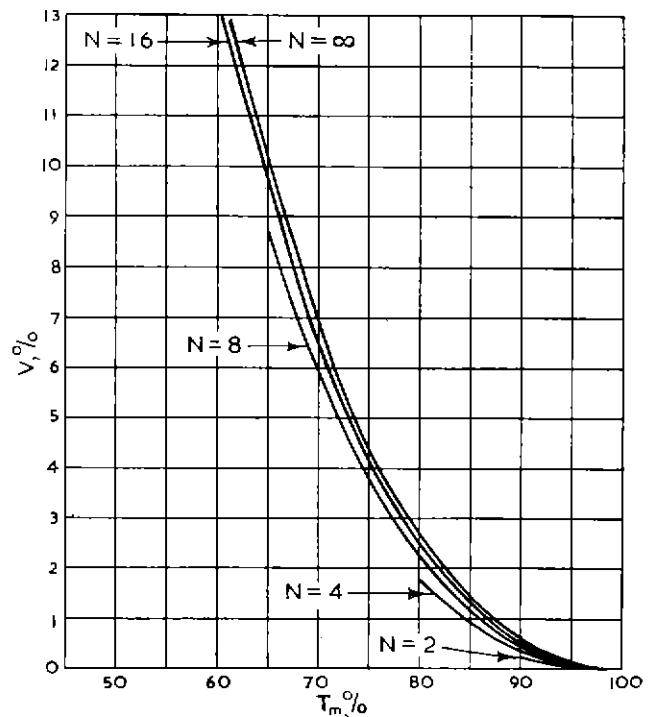


Fig. 7 — Theoretical relationship between the limiting veiling-glare index V and the transmission factor T_m for 2, 4, 8, 16, and ∞ glass/air interfaces

4.2 Quality Index for Lens Design

A more general expression for the veiling-glare index of a lens may be written (extending equation 4) as

$$V = K \left\{ 1 - \frac{N^N T_m^{N-1}}{[1 + (N-1)T_m]^N} \right\} + A \dots \dots (6)$$

where K is a numerical factor which depends on the particular design and construction of the lens. A is that component of the measured veiling-glare index which is due to the scattering of light by surface irregularities. For a lens which has 'clean' glass/air interfaces (unusual, unfortunately) A is small. Veiling-glare measurements on more than twenty lenses (differing in focal length, aperture, and make) show that K is less than unity. This evidence supports the view that equation 6 with $K=1$ represents an upper limit for V . If the design of a particular lens is good from the standpoint of secondary flare, then the value of K will be small and, if poor, K will approach unity. Hence an index of quality, Q , for lens design might be conveniently given by

$$Q = 1 - K$$

Since K is independent of the transmission factor T_m , we may use it, for instance, to estimate the improvement in veiling-glare index due to 'blooming' the glass/air interfaces of a multi-element lens.

In practice, experiments² other than a simple measurement of V are necessary in order to determine the value of A in equation 6.

5. Results

5.1 Veiling-glare Index

Using the method described in Section 2, the veiling-glare indices of twenty-one lenses, typical of those used for television, have been measured. The lenses, differing in design or make, had focal lengths ranging from 1 in. to 6 in. (25 mm to 150 mm), and had between four and sixteen glass/air interfaces. The lenses were measured at their maximum apertures, and the front and rear external lens surfaces were free from dust and fingerprints. The results are shown in Fig. 8, where each plotted point indicates the measured veiling-glare index and axial transmission of one lens. The broken line in the figure is the theoretical, upper limiting curve for a 'clean' lens having sixteen reflecting surfaces. It will be seen that the great majority of the points lie beneath the limiting curve. The mean veiling-glare index for this 'sample' of lenses is 1.4 per cent and the mean axial transmission is 80 per cent.

5.2 Effect of Aperture on the Veiling-glare Index

An experiment was carried out, using a set of four camera lenses designed for use with 16 mm film, in order to determine the effect on the veiling-glare index of stopping down a lens. The lenses had focal lengths of 25 mm, 37.5 mm, 50 mm, and 75 mm, with maximum apertures of $T/2^*$ except for the 75 mm lens which had a maximum aperture of $T/2.8$. The results are shown in Table 1.

*The effective aperture of a lens, taking account of the transmission factor, may be expressed as a $T/$ number, equivalent to the number of a lens possessing 100 per cent transmission.

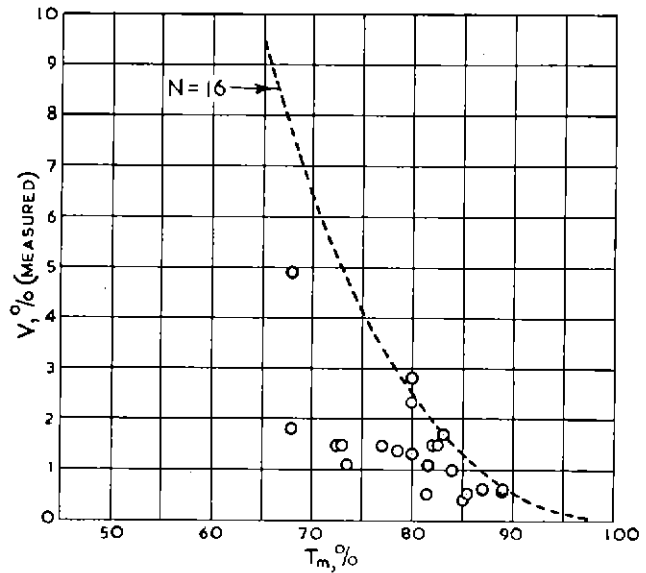


Fig. 8 — Results of veiling-glare and axial transmission measurements on a sample of twenty-one camera lenses ——— theoretical limiting curve for a lens with sixteen glass/air interfaces

The lenses with longer focal lengths (50 mm and 75 mm) appear to have substantially the same veiling-glare performance at all apertures from $T/2$ to $T/11$. There is a tendency for the index to rise at $T/11$ for the short focal length lenses. Measurements of this kind on other types of lenses also indicate that the veiling-glare index tends to increase slightly as the lens is stopped down. Kuwabara² has reported that this increase in veiling-glare with diminishing aperture is accentuated when dealing with small object-fields. It is interesting to note that this effect is reversed for primary flare (i.e. aberration flare), where stopping down the lens usually produces a marked improvement in detail contrast.

TABLE I

Focal length	Veiling-glare Index (%)			
	$T/2$	$T/2.8$	$T/5.6$	$T/11$
25 mm	2.6	—	2.5	3.2
37.5 mm	1.8	—	1.8	2.0
50 mm	1.8	—	1.7	1.9
75 mm	—	1.6	1.7	1.6

6. Distribution of Flare Light in the Image Plane

6.1 Method of Investigation

A lens was set up as for a normal veiling-glare measurement. Then, with the square black patch in position, the galvanometer readings were recorded as a vertical black

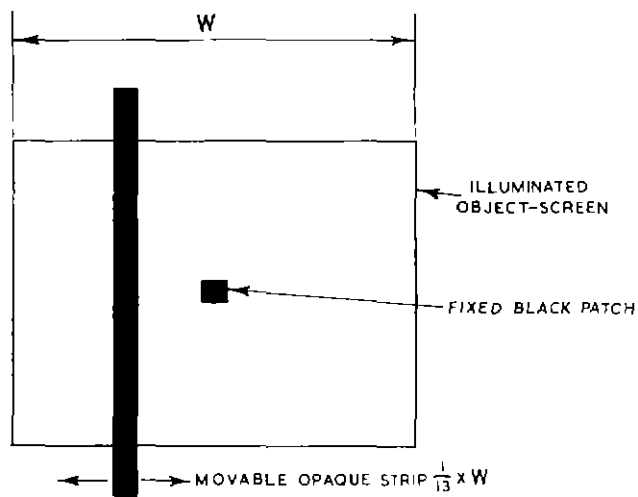


Fig. 9 — Method of measuring the distribution of secondary flare

strip (one-thirteenth of the width of the object-screen) was moved to obscure successive strips of the object-screen as indicated in Fig. 9. In effect, therefore, the object-screen was divided into thirteen strips and the contribution by each strip to the veiling-glare at the centre was determined. It will be apparent that the vertical black strip reduces the galvanometer reading by an amount which is proportional to the contribution to the total veiling-glare produced by the obscured element of the object-screen. The square black patch was then moved to the edge of the field and the experiment repeated. A subsidiary measurement of the normal brightness distribution across the object-screen was made by scanning it directly with a slit-photocell combination of small numerical aperture. This enabled the results of the main experiment to be corrected for the slight non-uniformity of the object-screen brightness.

6.2 Results

Figs. 10(a) and (b) show the results for two lenses. Fig. 10(a) relates to a telerecording lens of 2 in. (50 mm) focal

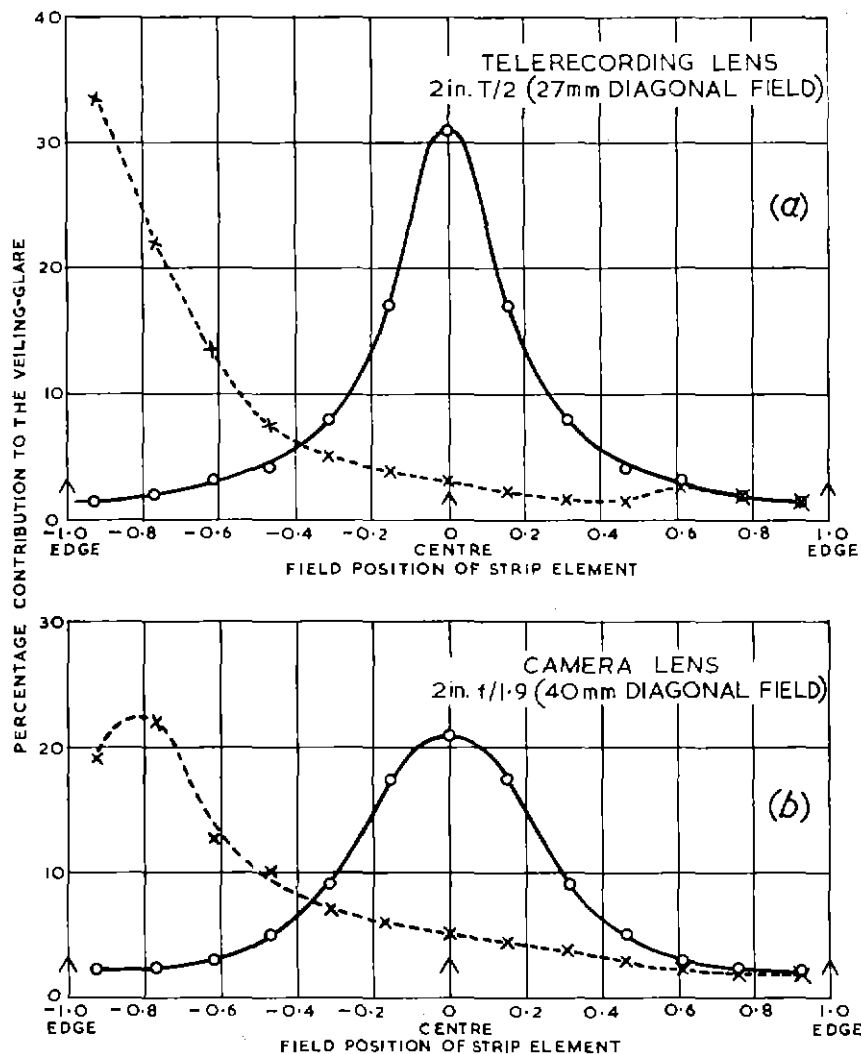


Fig. 10 — Contribution to the veiling-glare index by successive zones of the object-field

length at an aperture of $T/2$, which was designed for use with 35 mm film. Fig. 10(b) relates to a camera lens of similar focal length and aperture but used with a 40 mm diagonal format.

The results indicate a roughly 'Gaussian' type of non-uniform distribution of secondary flare light. The flare 'spread' associated with a small illuminated object-patch appears to extend over most of the image format and is always centred around the image position in the format. The width at half amplitude of the distribution is of the order of one-fifth to one-third of the format width.

7. Surface Dust and Fingerprints

7.1 Method of Investigation

A lens was mounted on an optical bench and arranged to produce an aerial image of an object-screen which was of the form shown in Fig. 11. The aerial image was scanned by means of a pinhole-photomultiplier combination whose effective aperture was larger than that of the lens. The direction of the scan was across the middle of the 'black' sectors of image, i.e. along the line AA' in Fig. 11. The relative flare intensity profile along this locus of the image was determined from the recorded output of the photomultiplier during the scan.

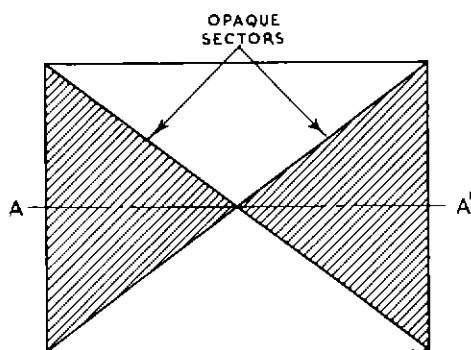


Fig. 11 — Object-screen arrangement for investigating secondary flare due to dust and fingerprints

7.2 Results

The lens used for the investigation was a camera lens of 2 in. (50 mm) focal length and aperture $f/4$ having eight glass/air interfaces. The results are given in Fig. 12 where the flare intensity in the image plane relative to that of peak white is plotted on a logarithmic scale against the position along the line of scan. Curve A was obtained when the lens was 'clean'. Curve B refers to the same lens after a thin layer of dust had been deposited on the surface of the front element. Curves C and D, respectively, indicate the changes due to a small fingerprint and a large thumbprint on the front element. It is clear from these results that greasy organic deposits, such as fingerprints, on the glass/air surfaces of a lens produce a more serious and extensive increase in flare than small amounts of natural dust.

7.3 Earlier Results with Dust Layers

Some earlier results are worth reporting. These relate to a set of camera lenses that had been stored for some

years unprotected and had accumulated rather thick layers of dust on their external glass/air surfaces. These were measured for normal veiling-glare index before and after cleaning the dusty surfaces. The details are shown in Table 2.

There is no doubt that surface irregularities of any description, even on only one surface, cause an increase in secondary flare which can far outweigh that due to specular interfacial reflections.

TABLE 2

Focal length	Veiling-glare Index at Full Aperture (%)	
	Before cleaning	After cleaning
50 mm	6.0	2.4
75 mm	8.0	1.5
100 mm	2.5	0.55
150 mm	2.9	1.5

8. Conclusions

1. Flare light from a small illuminated object-patch is distributed around the image of the patch in a non-uniform manner. The radial intensity distribution is somewhat 'Gaussian' in shape and extends, effectively, over a considerable area of the image format. The integrated result obtained when bright areas are well distributed over the whole of the object-field is a substantially uniform veil of flare light over the image format. When the whole of the object-field is uniformly illuminated the intensity of the veil relative to that of the image is used as a measure of the secondary flare performance of the lens. At present the performance in respect of flare of lenses for use with BBC television cameras is specified³ in terms of the veiling-glare index measured by the method described in Section 2.
2. Measurements on an arbitrary 'sample' of twenty-one different camera lenses gave a mean axial transmission of 80 per cent and a corresponding veiling-glare index of 1.4 per cent, with a patch of approximately 30 by 30 picture elements square.
3. An approximate general expression for the veiling-glare index, V , is given by

$$V = K \left\{ 1 - \frac{N^N T_m^{N-1}}{[1 + (N-1)T_m]^N} \right\} + A$$

where N is the number of glass/air interfaces and T_m is the transmission factor. K is a positive parameter usually less than unity. It is a constant for a given lens design and is independent of T_m . A is that component of the veiling-glare index which is due to surface irregularities. It too is independent of T_m .

4. Stopping down a lens tends to increase the veiling-glare index of short focal length lenses, but has little effect on other lenses.

5. Lens cleanliness is important. Surface irregularities of any description can cause a serious increase in secondary flare. Fingerprints appear to be more disastrous than natural dust layers, although both can easily outweigh the amount of secondary flare due to specular interfacial reflections.
6. It might be thought worth while in some instances to correct electronically for the frequency response dis-

tortion due to secondary flare, and a partial correction is certainly possible. On the other hand, lens manufacturers are becoming increasingly aware of this aspect of lens construction: considerable reductions in the present values of veiling-glare indices can be obtained by paying attention to the surface treatment and cementing of the lens elements, and also by adopting improved 'blooming' techniques.

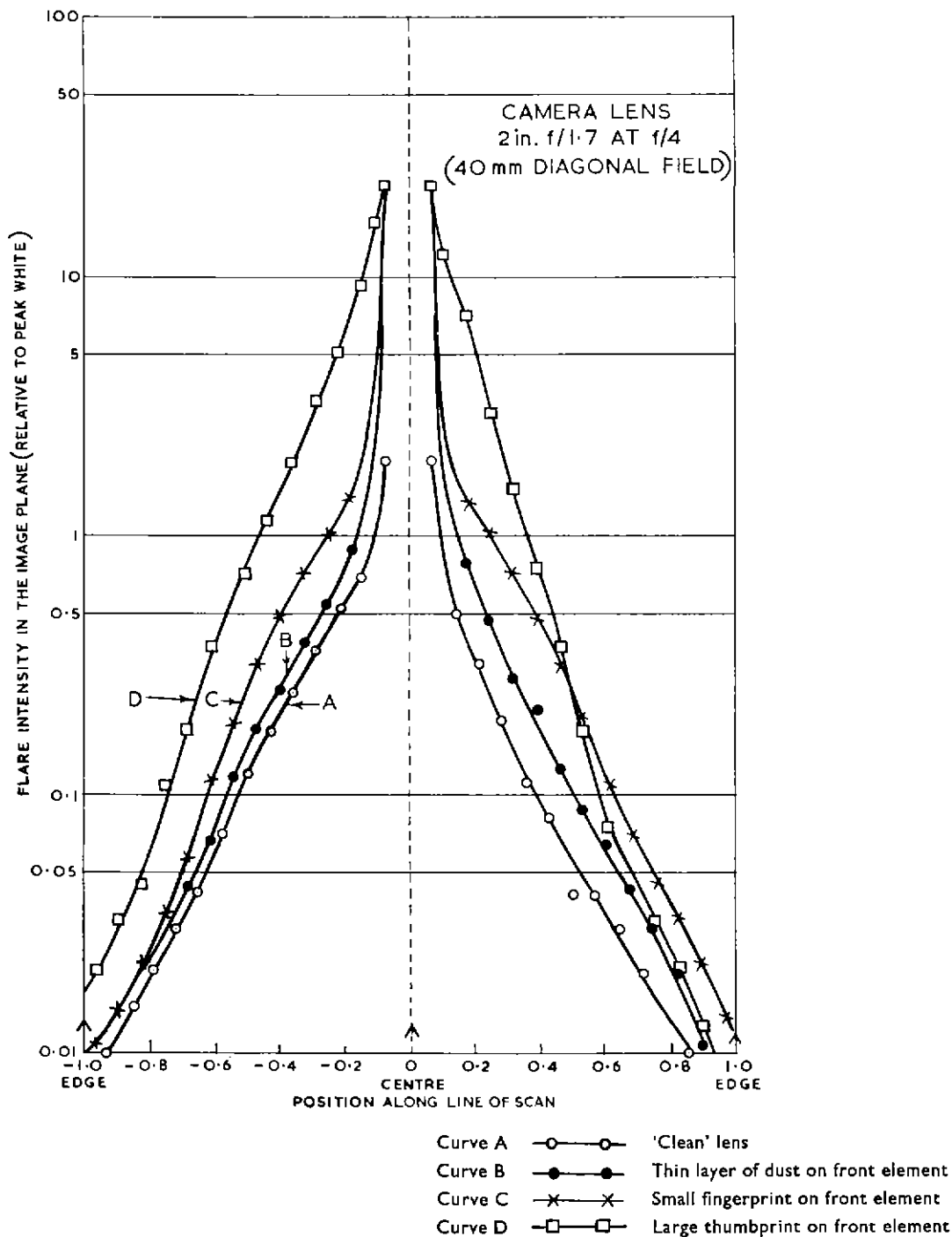


Fig. 12 — The effect of dust and fingerprints on the 'spread' and intensity of secondary flare

THE DESIGN OF LENS HOODS

SUMMARY

The factors which control the performance of a lens hood are discussed. A distinction is made between two degrees of protection given against unwanted light sources. Some numerical results are given which apply to the image orthicon television camera.

9. Introduction

The definition of veiling-glare index quoted in Part I and used in the BBC lens specification³ relates to a peak white level of illumination filling, but not exceeding the working field of view. This is unlikely to be true in any practical situation, but the assumption has been made that it is possible to use lens hoods which are efficient in preventing extraneous non-image-forming light from reaching the lens. The extent to which it is practicable to do this has been investigated and forms the subject of this monograph. Many lens hoods which are sold with photographic cameras are almost useless and it is not surprising that the value of lens hoods has been questioned by some enthusiastic amateurs.

10. Basic Considerations

10.1 Length of Hood

In Fig. 13, OX represents the optical axis of a lens and AB is the entrance pupil.* Rays from a point on the periphery of the field of view are inclined at an angle θ to the optical axis: three such rays are shown as AC, OD, BE. It is assumed that the object point is sufficiently distant that the three rays are nearly parallel. A section of lens hood is shown as LMF. A ray of light BF inclined at an angle ϕ to the optical axis will just touch the entrance pupil: this represents the limiting case because light from any source inclined at an angle greater than ϕ will not reach the entrance pupil AB. The locus of extreme positions of the aperture of the hood is given by the line AC, because the lens hood must cause no vignetting.

* Entrance pupil is defined as the image of the iris as seen through those components of the lens in front of the iris.

Let $AB = D$ (diameter of entrance pupil)
 $LM = L$ (length of hood)
 Then it can easily be shown that
 $L = D / (\tan \phi - \tan \theta) \dots \dots \dots (7)$

This expression gives the length of hood (measured from the plane of the entrance pupil) which is required for protection from a source inclined at an angle ϕ . Fig. 13 shows that as the point F moves along AC in the direction of C, the angle ϕ will diminish, i.e. the longer the hood, the better the protection.

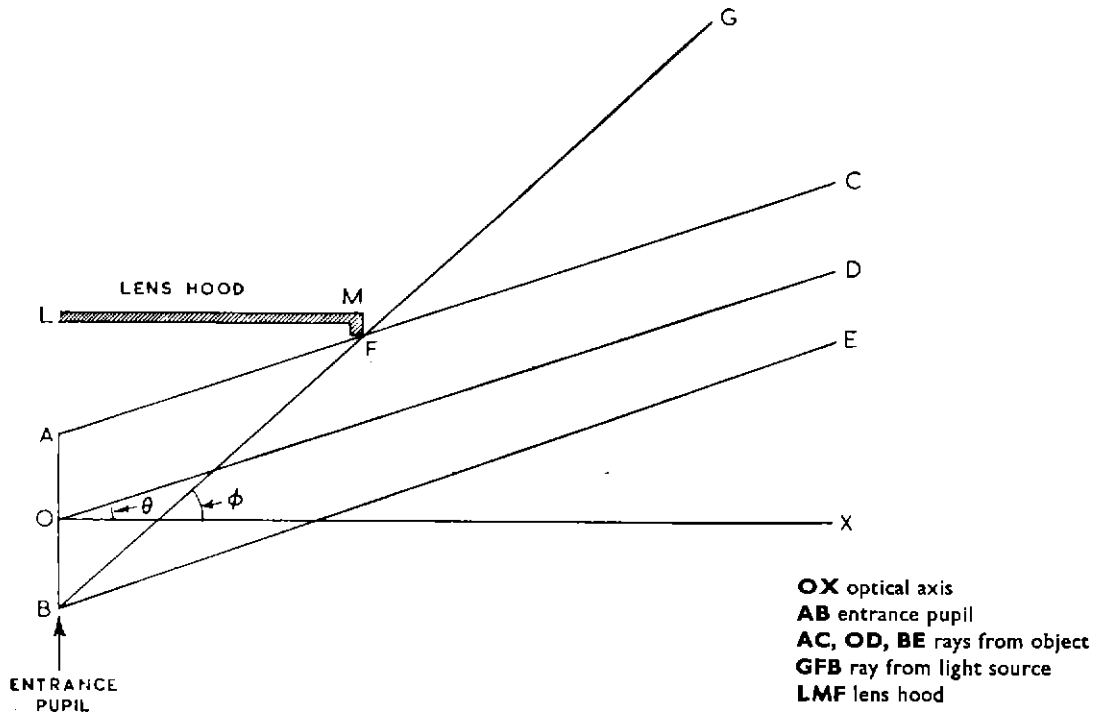


Fig. 13 — The action of a lens hood

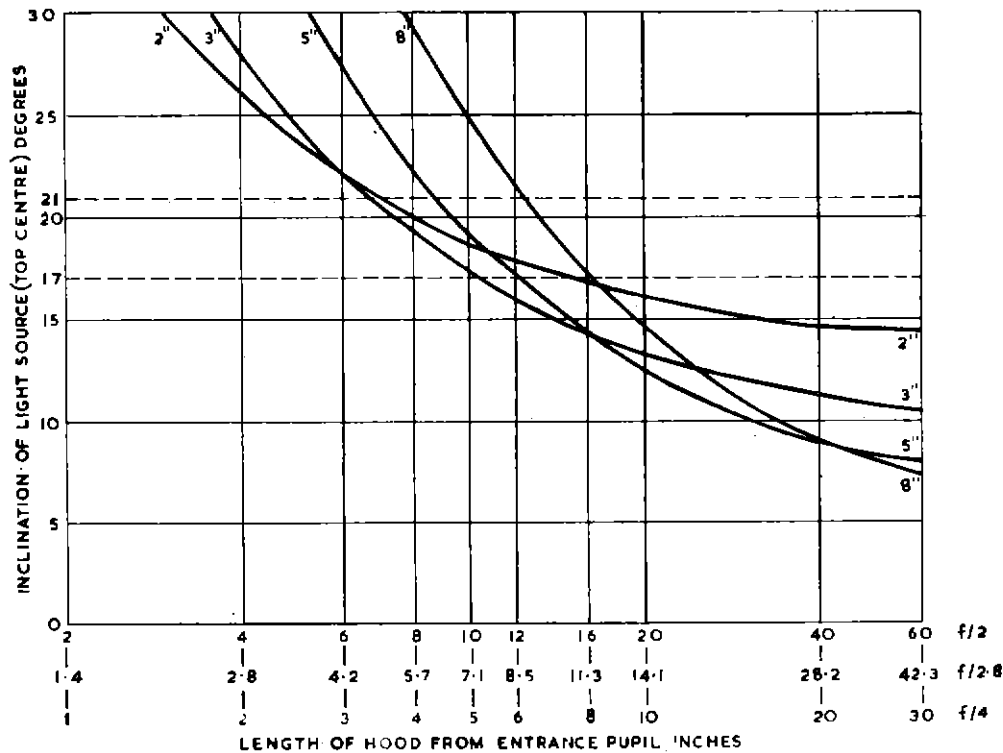


Fig. 14 — Rectangular lens hoods for 2 in.—8 in. lenses at apertures of $f/2$, $f/2.8$, and $f/4$ (Image size 0.96 in. by 1.28 in.)

10.2 Partial and Complete Protection

The protection given by a hood is not complete if non-image forming light reaches any part of the front element of the lens. Nevertheless, if the shadow cast by a lens hood from the offending light source just includes the whole of the entrance pupil (as represented by the area BFL in Fig. 13), then there is a very substantial reduction in the non-image-forming light which can be scattered in such a direction as to pass through the iris and finally reach the image. This condition is referred to as partial protection in the monograph.

For a lens operating at full aperture, this distinction between complete protection of the front element and shadowing of the entrance pupil becomes somewhat academic (although the plane of the entrance pupil will certainly not coincide with any part of the outside surface of the front element). Equation 7 gives the conditions for complete protection if D is the diameter of the front element and L is measured from the front element.

10.3 Shape of Lens Hood

The optimum shape of the front aperture of a lens hood is in general a rectangle with radiussed corners. The reason for this will be appreciated if the envelope of all the image-forming rays leaving the scene (which can be idealized as a rectangle perpendicular to the optical axis) and reaching the circular entrance pupil of the lens is considered. In its two extreme conditions we have a circle and a rectangle: at all intermediate planes we have a combination of these two shapes, namely a rectangle with modified corners

which are arcs of a circle. In designing lens hoods to work with television cameras, a considerable variation in the focal lengths is encountered. For example, an image orthicon may be used with a 2-in. lens and a 40-in. lens. The physical length of the hood considered as a multiple of the focal length is one of the factors which controls the shape of the aperture in the lens hood; the other factor is the angular field. Two specific examples may be helpful. For a 2-in. lens operating at $f/4$ and a hood giving partial protection from a light source immediately above the centre of the field and inclined at an angle of 17° , reference to Fig. 14 shows that a hood of about $7\frac{1}{2}$ in. length is required. A simple calculation shows that the front aperture of such a hood will be 4.1 in. by 5.3 in. with circular corners of radius 0.25 in. (the radius of the entrance pupil). In this case the front aperture is almost of rectangular shape. On the other hand, if we consider a 40-in. $f/8$ lens, a hood of length 9.6 in. will protect the lens from a light source above the centre of the field inclined at an angle of 28° . The shape of the front aperture is now almost circular. The rectangle has dimensions 5.23 in. by 5.31 in. and the radius of curvature of the rounded corners is $2\frac{1}{2}$ in.

The above two examples are perhaps somewhat extreme cases but they show that somewhere in the range of focal lengths between 2 in. and 40 in. (and for hoods of the order of 10 in. long) the shape of the front aperture of the hood changes from almost rectangular to almost circular. In specifying hoods* for the image orthicon camera it has

*BBC Specification TV88/2.

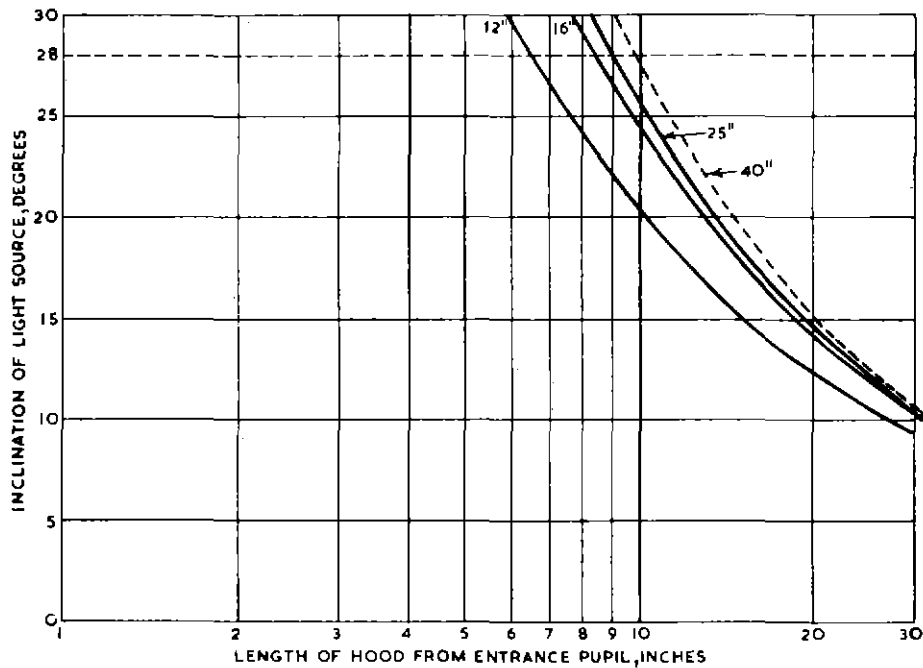


Fig. 15 — Conical lens hoods for 12 in.—40 in. lenses relative apertures not constant 12 in. $f/4$, 16 in. $f/4$, 25 in. $f/5.6$, and 40 in. $f/8$. (Image size 0.96 in. by 1.28 in.)

been decided to fit lenses with focal lengths up to and including 8 in. with hoods with a rectangular aperture but for focal lengths of 12 in. and greater a circular aperture is a sufficiently good approximation to the optimum shape for most practical purposes.

11. Protection Angles

In the two examples just quoted, arbitrary protection angles were given without any explanation. If each lens was used in isolation (not mounted on a lens turret) and there were no restrictions on the length of lens hood, then it would be possible to shield the entrance pupil from light sources that were only just outside the field of view. The graphs given in Fig. 14 show that a law of diminishing returns operates in the sense that for each extra (angular) degree of protection, the increments in length increase rapidly. As an example, we may note that the top centre of the field of a 2-in. lens (image orthicon field) subtends an angle of about $13^{\circ} 30'$ ($\arctan 0.24$) and for protection against light sources at 20° , 18° , 16° , 14° we find from equation 13 (or Fig. 14) that lengths of hood for an aperture of $f/4$ are 4, 5.9, 10.7, and 53.6 in. respectively. Alternatively we may observe that on differentiating equation 1, we have

$$\frac{dL}{d\phi} = -D \frac{\cos^2 \theta}{\sin^2(\theta - \phi)} \dots \dots \dots (8)$$

The modulus of this function increases very rapidly as ϕ tends towards θ .

Because a hood 53.6 in. long would be very inconvenient to use (its front aperture would be about $26\frac{1}{2}$ in. by 35 in.) and difficult to make with sufficient stability* for a

* If the front aperture of the hood is not accurately positioned, an image of the hood is formed which is substantially in focus.

reasonable weight, clearly a compromise must be sought. In actual fact, turret working is almost invariably used with television cameras† so that the maximum length of hood is restricted because of the necessity of avoiding interference between the field of the lens in use and any parts of the mounts (including hoods) of the other lenses on the turret. However, the above considerations show that even if turret working was not usual, it would be necessary to restrict the angle of protection.

Detailed design considerations relating to one specific camera would be inappropriate in this monograph but it may be of general interest to state that the latest versions of the image orthicon television camera use a turret of diameter such that it is possible to protect the lenses in the 2 in. to 8 in. range of focal lengths (aperture not exceeding $f/4$) for light sources inclined at an angle of 17° above the optical axis in a vertical plane. This gives rise to hoods which are in the range of lengths from $5\frac{1}{2}$ in. to $8\frac{1}{2}$ in. (see Fig. 14) and this can be done without causing any mutual interference of one lens with another. A comparison of the light shielding properties of conical and rectangular hoods of the same length is shown in Figs. 16a and b. This diagram also shows the nature of the protection in planes other than the vertical plane which includes the optical axis.

12. Effect of Unusual Lens Designs

The simple theory of hoods embodied in equation 1 will require considerable modification to suit telecentric‡ designs and those which are more than telecentric. One

† Except when the television camera uses a zoom lens.
‡ A lens is said to be telecentric when either the entrance or exit pupil is located at infinity.

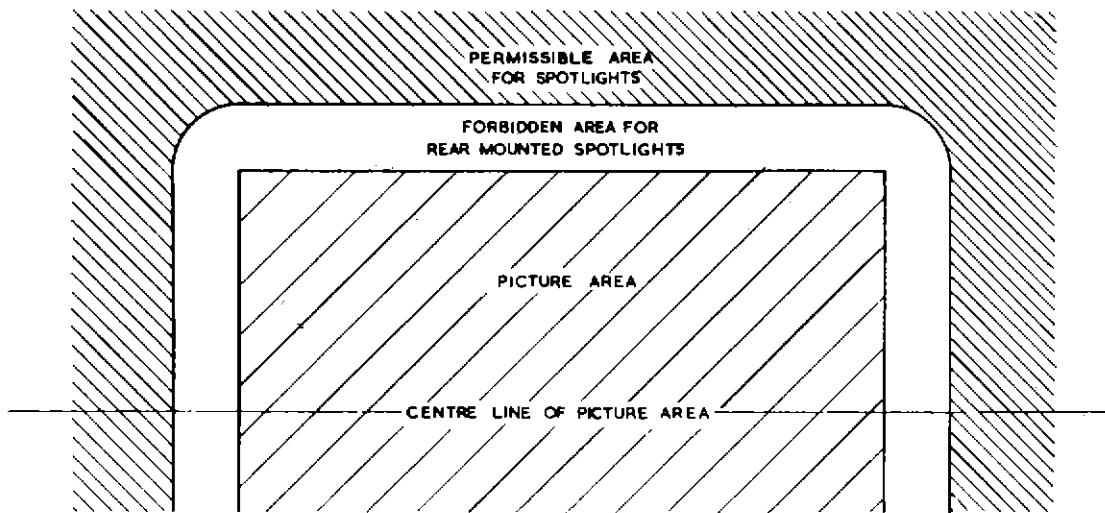


Fig. 16a — The effect of using a rectangular hood, $7\frac{1}{2}$ in. long, with a 2 in. lens (1.6 in. diagonal-image field)

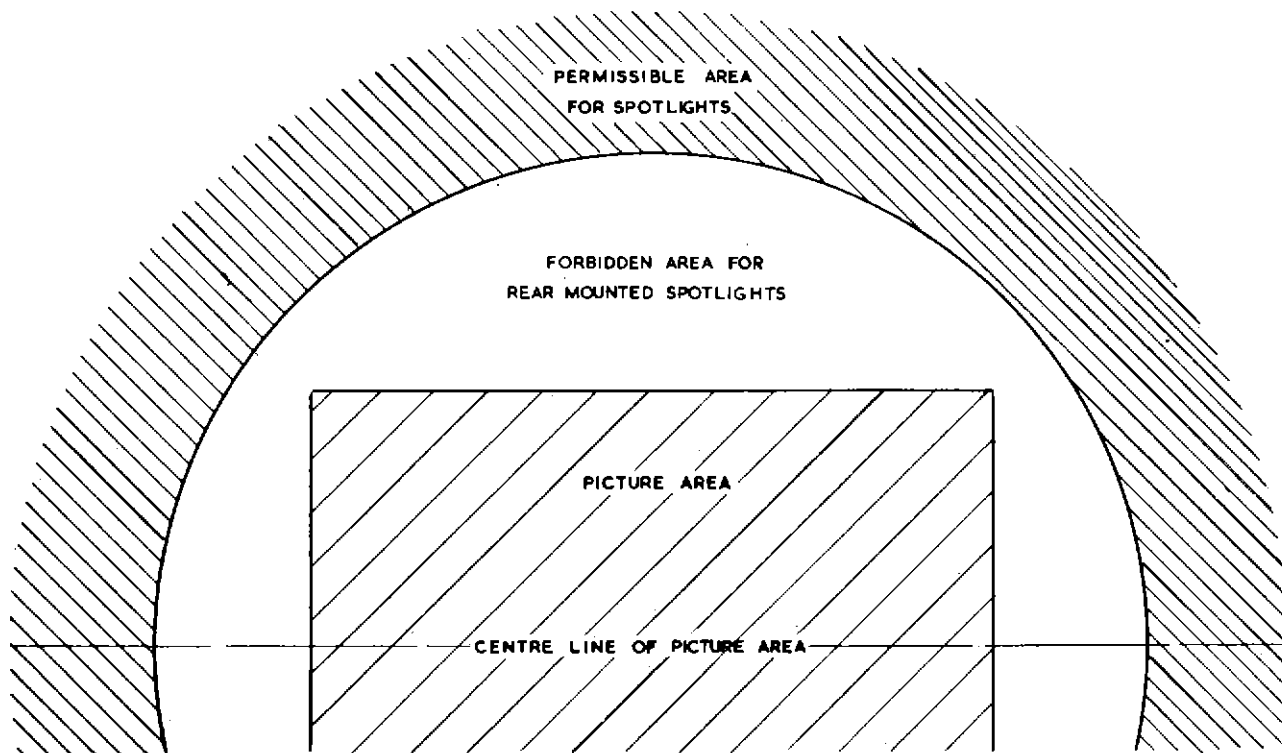


Fig. 16b — The effect of using a conical hood, $7\frac{1}{2}$ in. long, with a 2 in. lens (1.6 in. diagonal-image field)

result can be the disappearance of the distinction between partial and complete protection. This happens when the stop is external to the lens. Another factor which must be considered is the changing position of the entrance pupil with field angle. If the lens hood protects the entrance pupil (in all its positions) from stray light then a condition of partial protection will have been achieved although the data plotted in Figs. 14 and 15 may not be applicable. If the front element is protected by the hood then there will be a condition of 'complete protection' whatever the design of the lens.

13. Conclusions

1. For complete protection against light sources, no light from the sources in question must reach the front of the lens.
2. For a lens which is stopped down, a good measure of

protection is achieved if the hood just prevents unwanted light from reaching the entrance pupil.

3. To be really effective, lens hoods have to be long. Mutual interference between several lenses mounted on a turret is the factor which usually limits the length of hood and thus the protection angle.
4. The optimum shape of a lens hood is rectangular with radiussed corners. For television applications the optimum shape varies from almost rectangular to almost circular.

14. References

1. Guild, J., *Proceedings of London Conferences on Optical Instruments 1950*. Chapman and Hall, pp. 212 to 230.
2. Kuwabara, G., *On the Flare of Lenses*, J. Opt. Soc. Am., Vol. 43, p. 53, 1953.
3. BBC, *Specification for Television Lenses*, TV88/2.

